



Automatic Segmentation of Skin Melanoma Images Using Hybrid Method

Gurkirat Kaur, Er. Kirti Joshi

Department of Computer Science & Engineering, RIMT(IET) Mandi-Gobindgarh,
Punjab, India

DOI: [10.23956/ijarcsse/V7I2/0104](https://doi.org/10.23956/ijarcsse/V7I2/0104)

Abstract: Melanoma is a cancerous lesion in the pigment-bearing basal layers of the epidermis and is the most deadly form of skin cancer, yet it is also the most treatable, with a cure rate for early-stage melanoma of almost 100%. Therefore, there is a need to develop computer-aided diagnostic systems to facilitate the early detection of melanoma. The first step in these systems is skin lesion segmentation. The next essential step is feature extraction and pattern analysis procedures to make a diagnosis. According to the literature, pigment network or reticular pattern is an important diagnostic parameter for melanoma. We decided to work on this automatic melanoma detection system. In this work a brief study has been carried out about the existing segmentation methods adopted by different scholars and a neural network based method is presented for effective segmentation of the melanoma images. In previous work, various methods i.e. Region refinement, adaptive thresholding (AT), gradient vector flow (GVF), adaptive snake (AS); fuzzy-based split-and-merge algorithm (FBSM), k-nearest neighbor, k-means, log filtering etc. has been proposed for the segmentation of melanoma images but their drawback is improper segmentation and more complexity and calculation time. Our method uses testing and training property of neural networks in which a neural object has been created by training it with normal skin and lesion pixels and then same object is used for segmenting other images having similar intensity values. Experimental results shows better results in terms of accuracy values of final segmentation.

Keywords: skin cancer, Medical segmentation, ANN etc.

I. INTRODUCTION

Skin cancers are the most common form of cancers in humans [1]. The American Cancer Society estimates that more than 700 000 new skin cancers are diagnosed annually in the United States alone [2]. Skin cancers can be classified into melanoma and non-melanoma. Although melanomas are much less common than non-melanomas, they account for most of the mortality from skin cancers [2]. Detection of malignant melanoma in its early stages considerably reduces morbidity and mortality. Early detection also saves hundreds of millions of dollars that otherwise would be spent on the treatment of advanced diseases [3]. If cutaneous melanoma is detected in its early stages and removed, there is a very high likelihood that the patient will survive [4,5]. Clinical features of pigmented lesions suggestive of melanoma are what are known as the ABCDs of melanoma [3]: asymmetry, border irregularity, color variegation, and diameter greater than 6 mm. Image analysis techniques for measuring these features have been developed [6]. Measurement of image features for diagnosis of melanoma requires that first the lesions be detected and localized in an image. It is essential that lesion boundaries are determined accurately so that measurements, e.g. maximum diameter, asymmetry, irregularity of the boundary, and color characteristics can be accurately computed. For delineating lesion boundaries, various image segmentation methods have been developed. These methods use color and texture information in an image to find the lesion boundaries. To segment a skin image into lesions, Umbaugh et al. [7] transformed the RGB color space into a spherical color space with coordinates defined by quantizing the AB space into four colors, they were then able to partition a color image into different regions and isolate lesions from the background. In a separate study, Umbaugh et al. [8] developed a principal-components transform in a userselected color space to segment skin cancer images. Green et al. [9] segmented a color image by first finding the average color of a small area of a lesion and the average color of a small area of the background interactively. Then, by mapping the image colors to the vector connecting the two average colors, they obtained a histogram.

The color corresponding to the valley between the two peaks in the histogram was then used as the threshold value to segment the image. Dhawan and Sicsu [10] used image gray values and textures separately to segment skin images. They then combined the results to obtain the lesion boundaries. Hance et al. [11] compared the accuracy of six different color segmentation techniques, and found that when two or more of the techniques are combined, accuracy that is considerably higher than the accuracy of any one of the individual techniques will be obtained [12]. Dermoscopic images have great potential in the early diagnosis of malignant melanoma, but their interpretation is time consuming and subjective, even for trained dermatologists [13]. Therefore, there is currently a great interest in the development of computer-aided diagnosis systems that can assist the clinical evaluation of dermatologists. The standard approach in

automatic dermoscopic image analysis has usually three stages: 1) image segmentation; 2) feature extraction and feature selection; and 3) lesion classification. The segmentation stage is one of the most important since it affects the accuracy of the subsequent steps. However, segmentation is difficult because of the great variety of lesion shapes, sizes, and colors along with different skin types and textures. In addition, some lesions have irregular boundaries and in some cases there is a smooth transition between the lesion and the skin. Other difficulties are related to the presence of dark hair covering the lesions and the existence of specular reflections.

II. NEED OF PREPROCESSING AND EXISTED SEGMENTATION TECHNIQUES

1. Preprocessing
2. Initial segmentation
3. Region refinement• adaptive thresholding (AT);
4. Gradient vector flow (GVF);
5. Adaptive snake (AS);
6. Fuzzy-based split-and-merge algorithm (FBSM).

2.1 Preprocessing

The first step in various image segmentation methods can be considered a preprocessing operation that transforms a color image into an intensity image. This operation is motivated by two observations: 1. Skin lesions come in a variety of colors; therefore, absolute colors are not very useful in segmenting images. However, changes in color from a lesion to its background (its surrounding healthy skin) are similarly observed in all images; therefore, changes in color can be used to effectively segment images. 2. When segmenting a skin image, significant color variations may exist within a lesion or in the background. Such variations should be suppressed since our interest is in color changes from the background to a lesion or from a lesion to the background.

Observation 1 suggests that one should use changes in color rather than absolute colors to segment images. Therefore, we transform pixel colors that are vector quantities into intensities that are scalars and represent color differences. Observation 2 states that, among the color changes, only those belonging to a lesion boundary are important in image segmentation, and color changes inside a lesion or in the background should be ignored. We transform our images that are in RGB color coordinates into images that are in CIELAB or CIE 1976 $L^*a^*b^*$ color coordinates [14]. CIELAB is a color space standardized by the CIE (Commission Internationale de l'Eclairage) in 1976 to measure color differences.

This is a uniform color space defined in such a way that Euclidean distance between two colors (defined as DE) is proportional to their visual difference. Color in the CIELAB space can be described with less redundancy than in the RGB space. RGB color coordinates can be transformed into $L^*a^*b^*$ color coordinates using the following formulae

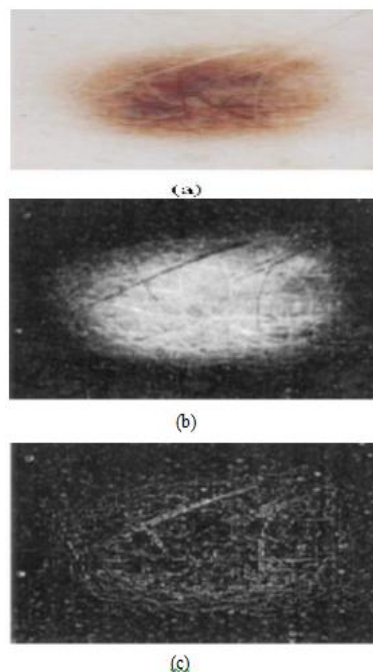


Figure 1: (a) A color image showing an atypical lesion. (b) Image obtained after mapping colors into intensities in such a way that the intensity at a pixel is proportional to the CIELAB color distance of the pixel to the color of the background. (c) Gradient magnitudes of (b) obtained by the Sobel operator. Larger gradients are shown brighter.

2.2 Initial segmentation

To reduce the effect of image noise and intensity variations due to skin's repetitive texture and hair, an image is first low-pass filtered before being segmented. Fig. 3(b) shows the image of Fig. 3(a) after being smoothed with a 2D Gaussian kernel of standard deviation 2 pixels. As can be observed, although smoothing reduce details in the image, the

smoothed image still contains information about the lesion, which is brighter than the background. The objective in the initial segmentation is to determine the approximate position and shape of a lesion, and then use double thresholding to narrow in on an image area where the optimal lesion boundary exists. Since the optimal threshold value at one boundary point may differ from that at another boundary point, the objective in double thresholding is to select a range of threshold values that includes the optimal threshold value at every boundary point. Double thresholding also reduces the number of noisy regions obtained as a result of intensity thresholding. Consider an image scanline, The horizontal axis shows pixels in the scanline, while the vertical axis shows the intensities of the pixels. As can be observed, if the threshold value is not selected properly, noisy regions from intensity variations in the lesion or background will be obtained. If there were no details from hair or skin texture, or if there were no intensity variations inside a lesion, a single threshold value T would have been sufficient to isolate a lesion from its background. However, since image variations from hair and skin texture usually exist in an image, a single threshold value may detect noisy regions from hair and skin texture. If such regions are close to each other, they may merge and create larger regions. By increasing the threshold value, we will observe that the number and size of noisy regions in the background will decrease.

If we decrease the threshold value, we will see that the number and size of noisy regions in the lesion will decrease. The use of two threshold values will, therefore, make it possible to obtain rather noise-free regions for both the lesion and background. Double thresholding will produce a segmentation that either will be free of noisy regions, or will contain fewer and smaller noisy regions than when a single threshold value is used. Double thresholding, however, requires the use of an initial threshold value.

2.3 Region refinement

The double thresholding process described in the preceding section determines an image area where a lesion boundary obtained from a range of threshold values will exist. Since the best threshold value in one local area may be different from the best threshold value in another local area, this range of threshold values is expected to include the best threshold value for all boundary pixels. We will assume that an optimal threshold value produces a boundary pixel that has a locally maximum gradient magnitude. Therefore, we will move an initial boundary pixel to the pixel in its neighborhood having a locally maximum gradient magnitude. Region boundaries in an image are best described by pixels with locally maximum gradient magnitudes [14– 17]. Pixels with locally maximum gradient magnitudes can be determined without any user interaction; therefore, the process is automatic. Locally maximum gradients in an image, however, not only represent lesion boundaries, they also represent small details inside and outside a lesion. In addition, an obtained boundary may merge with another boundary due to image noise and produce a false lesion boundary

2.4 Adaptive Thresholding

(AT) Lesion segmentation can be obtained by comparing the color of each pixel with a threshold. The pixel is classified as active (lesion) if it is darker than the threshold. The output of this step is a binary image. Morphological post-processing is then applied to fill the holes and to select the largest connected component in the binary image.

2.5 Gradient Vector Flow (GVF)

The GVF snake is a well-known algorithm proposed in [32] which has been successfully used in many medical imaging.

2.6 Adaptive Snake (AS)

Active contours are often attracted by spurious edges which do not belong to the lesion boundary. These normally appear in dermoscopic images due to artifacts such as hair, specular reflections or even from variations in the skin texture. Therefore, we need robust methods which are able to discard the influence of outlier edges. The adaptive snake tries to achieve this goal [22]. First, the method detects contour segments (strokes) in the image, using edge linking, and then approximates a subset of them using a robust estimation algorithm based on the expectation-maximization (EM).

2.7 Fuzzy-Based Split-and-Merge Algorithm (FBSM)

The sixth method used in this study is a fuzzy-based split-and-merge algorithm (FBSM), recently proposed in [17], [18]. The algorithm originally aims at unsupervised perceptual segmentation of natural color images. Since the algorithm has the significant advantage to stop the process at the specified number of segmented regions, it is applicable to the segmentation of dermoscopic images. First, the FBSM algorithm extracts color features and texture features from an original image. The values of L^* , A^* and b^* , and are used as color features, and the statistical geometrical features (SGF) [9] are used as texture features. Then, a split-and-merge technique is executed in four stages: simple splitting, local merging, global merging and boundary refinement. During the latter three stages, the similarity of any adjacent regions is estimated using the fuzzy-based homogeneity measure that combines the similarity of color features and texture features with different degrees of importance. The adoption of a fuzzy-based homogeneity measure simplifies the complex mechanism of integrating different features by means of symbolic representations.

III. PROPOSED METHOD

Early work on automated systems in detecting melanoma images assesses the risk of melanoma using dermoscopy images. These are images that are obtained via a digital derma scope, which is a device that assists dermatologists by magnifying surface detail and filtering surface reflectance. However, only 48% of practicing

dermatologists in the U.S. use derma scopes, so the proposed automated systems are difficult to widely adopt. Recent systems use images taken by a standard digital camera, which is more accessible to dermatologists. The photographs are segmented to identify the lesion area, features are extracted from the lesion, and the lesion is classified in terms of risk of melanoma. In this we have worked on images taken by normal cameras. The Various methods involved in the proposed work are as follows

3.1 Preprocessing

a. Collection of datasets

All the images were collected from the internet which includes photographs from random sites and journals.

b. Pre-processing the images

The images used are in jpg format while scanning and then converted to Lab format.

3.2 FCM clustering

FCM is a method of clustering which allows one piece of data to belong to two or more clusters. The main difference between the traditional hard clustering and fuzzy clustering can be stated as follows. While in hard clustering an entity resides only to single cluster, in fuzzy clustering entities are allowed to reside too many clusters with deferent degrees of membership. The most known method of fuzzy clustering is the Fuzzy c-Means method which is being most widely used in image processing applications. The steps involved in FCM are briefed as below. The following is description of the FCM algorithm, which is implemented Fuzzy Logic.

1. Select the number of clusters $c(2 \leq c \leq n)$, exponential weight $\mu(1 < \mu < \infty)$, initial partition matrix U^0 , and the termination criterion . Also, set the iteration index l to 0.
2. Calculate the fuzzy cluster centers $\{V_i^l \mid i = 1, 2, 3, \dots, c\}$ by using U^l
3. Calculate the new partition matrix U^{l+1} by using $\{V_i^l \mid i = 1, 2, 3, \dots, c\}$
4. Calculate the new partition matrix $\Delta = \|U^{i+1} - U^i\| = \text{MAX}_{i,j} |u_{i,j}^{i+1} - u_{i,j}^i|$. if $\Delta > \epsilon$ then set $i = i + 1$ and go to step 2. If , then stop.

3.3 Gaussian Mixture Model

A Gaussian Mixture Model (GMM) is a parametric probability density function represented as a weighted sum of Gaussian component densities. GMMs are commonly used as a parametric model of the probability distribution of continuous measurements or features in a biometric system, such as vocal-tract related spectral features in a speaker recognition system. GMM parameters are estimated from training data using the iterative Expectation-Maximization (EM) algorithm or Maximum A Posteriori (MAP) estimation from a well-trained prior model. The complete Gaussian mixture model is parameterized by the mean vectors, covariance matrices and mixture weights from all component densities. GMMs are often used in biometric systems, most notably in speaker recognition systems, due to their capability of representing a large class of sample distributions. One of the powerful attributes of the GMM is its ability to form smooth approximations to arbitrarily shaped densities. The classical uni-modal Gaussian model represents feature distributions by a position (mean vector) and a elliptic shape (covariance matrix) and a nearest neighbor model represents a distribution by a discrete set of characteristic templates. A GMM acts as a hybrid between these two models by using a discrete set of Gaussian functions, each with their own mean and covariance matrix, to allow a better modeling capability.

3.4 Artificial neural network

The multi-layer back-propagation neural network is best suited for the engineering applications. Many researchers proved that the multi-layer back propagation with three layers can perform arbitrarily complex classification [17].

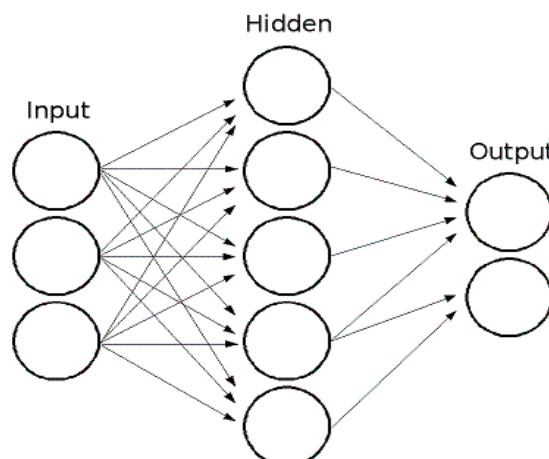


Figure 2: Three layers model back propagation neutral network

Propagation of data takes place from input layer to the output layer. In supervised learning the network is presented with a series of matched input and output patterns and the connection strengths or weights of the connections automatically adjusted to decrease the difference between the actual and desired outputs. Patterns are presented to the network and a feedback signal which is equal to the difference between the desired and actual output is propagated backwards through the network for the adjustment of weights of the layers' connections according to the back propagation learning algorithm. `trainlm` is a network training function that updates weight and bias values according to Levenberg-Marquardt optimization. `trainlm` is often the fastest backpropagation algorithm in the toolbox, and is highly recommended as a first-choice supervised algorithm, although it does require more memory than other algorithms.

IV. RESULTS

In this section experimental result has been shown for the proposed automatic system created for inspection of pigmented skin lesions and for discriminating between malignant area and normal skin. The results have been visualized in terms of tables figures and graphs. In this paper results has been shown for single image but experiment has been performed on number of images. The input image that has been used for training the neural object has been shown below along with output of the algorithm at various steps.



Figure 3: Input melanoma Image

Then fuzzy clustering has been carried out to get the texture representatives. The output of FCM has been shown below

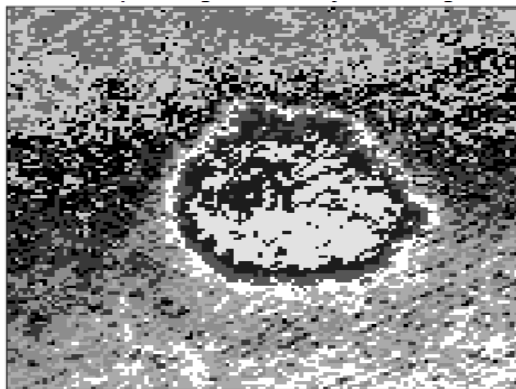


Figure 4: results after applying fuzzy clustering

The next step is post segmentation of the image using Gaussian mixture models created by texture representatives obtained above. The results of GMM analysis has been shown below

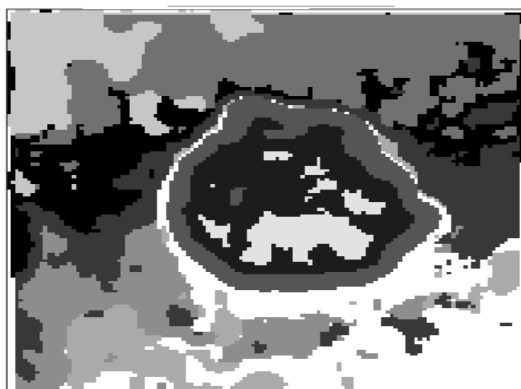


Figure 5: Segmentation results after GMM modeling

After Gaussian modeling whole figure is divided into two parts, one is pure lesion region and the other is skin region. This has been chosen according to maximum negative log likelihood values as they contain the darkest skin lesion regions. The final segmentation obtained by ANN has been shown below.

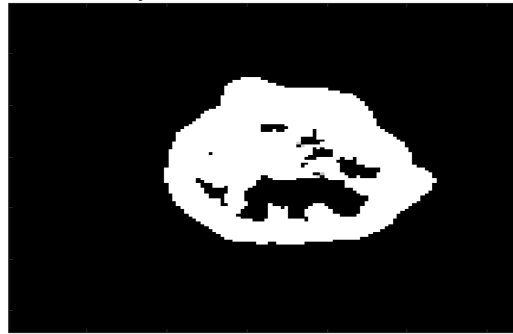


Figure 6: Segmentation after ANN where white pixels represent defected area and black as un-defected area

After this RGB values from two corresponding classes are concatenated separately and make ready to feed in neural network for training process



Figure 6: Final segmentation done using trained neural object

As we can see that Ann gives far better results in final segmentation and gives high accuracy rates which is specified by sensitivity and specificity values. The results of other images segmented using same neural object has been shown below.

Table 1: Defines sensitivity and specificity parameters for evaluating accuracy

Melanoma image	True Positive	False Negative	True Negative	False positive	Sensitivity value	Specificity value
Image1	8142	625	36561	536	0.9287	0.9856
Image2	3831	185	3226	238	0.9539	0.9927
Image3	8142	2625	14972	788	0.9287	0.9500
Image4	44274	44	36561	536	0.9990	0.9856

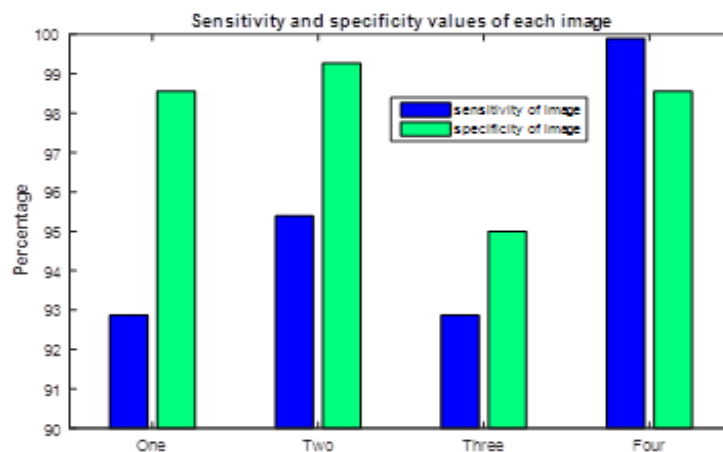


Figure 7: Sensitivity and specificity values visualized by bar graphs

V. CONCLUSION

Different literature work address the problem of how to determine the absence or presence of pigment networks in a given dermoscopic image. Some define it as a typical pigment network is which is light-to-dark brown in color with small, uniformly spaced network holes and thin network lines distributed more or less regularly throughout the lesion and usually thinning out at the periphery. Most of the methods are robust, reliable, computer-aided diagnostic tool for analyzing the texture in lesions of the skin to detect pigment networks in the presence of other structures such as dots. All these methods have some drawbacks, in which methods are defined according to a particular feature of the melanoma image such as intensity, streaks and their regularity and non-regularity characteristics. Different methods used different methods for extraction of feature set as well as final classification in terms of present or absent of the melanoma cancer in the image. In this work we have proposed a testing and training based method in which first a neural object has been produced by training it with two classes of defected melanoma portion and non-defected melanoma portion an then various images of similar intensity can be segmented using this trained neural object. It decreases calculation time for segmentation along with better accuracy results. In this we used fuzzy clustering and Gaussian models for pre-segmentation of normal skin and lesion region. After then ANN is applied for final segmentation of the images. This method works pretty well in most of the cases of skin cancer images but does not differentiate melanoma cancer images from images having other skin problems i.e. eczema etc. Therefore in future a property oriented research can be done which can include the features of melanoma images and use them for differentiating the images from other skin deceases.

REFERENCES

- [1] A.W. Kopf, T.G. Salopek, J. Slade, A.A. Marghood, R.S. Bart, Techniques of cutaneous examination for the detection of skin cancer, *Cancer Supplement 75 (2)* (1994) 684–690.
- [2] D.E. Elder, Skin cancer: Melanoma and other specific nonmelanoma skin cancers, *Cancer Supplement 75 (1)* (1994) 245–256.
- [3] NIH Consensus Conference, Diagnosis and treatment of early melanoma, *JAMA 268 (10)* (1992) 1314–1319.
- [4] A.J. Sober, T.B. Fitzpatrick, M.C. Mihm, Early recognition of cutaneous melanoma, *JAMA 242* (1979) 2795–2799.
- [5] M.M. Wick, A.J. Sober, T.B. Fitzpatrick, Clinical characteristics of early cutaneous melanoma, *Cancer 45* (1980) 2684–2686.
- [6] W.V. Stoecker, W.W. Li, R.H. Moss, Automatic detection of asymmetry in skin tumors, *Computerized Medical Imaging and Graphics 16 (3)* (1992) 191–197.
- [7] S.E. Umbaugh, R.H. Moss, W.V. Stoecker, Automatic color segmentation of images with applications in detection of variegated coloring in skin tumors, *IEEE Engng Med. Biol.* 8 (1989) 43–52.
- [8] S.E. Umbaugh, R.H. Moss, W.V. Stoecker, An automatic color segmentation algorithm with application to identification of skin tumor borders, *Computerized Medical Imaging and Graphics 16 (3)* (1992) 227–235.
- [9] A. Green, N. Martin, J. Pfitzner, M. O'Rourke, N. Knight, Computer image analysis in the diagnosis of melanoma, *J. American Academy of Dermatology 31 (6)* (1994) 958–964.
- [10] A.P. Dhawan, A. Sicsu, Segmentation of images of skin lesions using color and texture information of surface pigmentation, *Computerized Medical Imaging and Graphics 16 (3)* (1992) 163–177.
- [11] G.A. Hance, S.E. Umbaugh, R.H. Moss, W.V. Stoecker, Unsupervised color image segmentation with application to skin tumor borders, *IEEE Engineering in Medicine and Biology 15 (1)* (1996) 104–111 [12]G. Argenziano, H. P. Soyer, V. D. Giorgio, D. Piccolo, P. Carli, M. Delfino, A. Ferrari, R. Hofmann-Wellenhof, D. Massi, G. Mazzocchetti, M. Scalvenzi, and I. H.Wolf, *Dermoscopy, An Interactive Atlas EDRA Medical Publishing, 2000* [Online]. Available: <http://www.dermoscopy.org>
- [13] M. Binder, M. Schwarz, A. Winkler, A. Steiner, A. Kaider, K. Wolff, and M. Pehamberger, “Epiluminescence microscopy. A useful tool for the diagnosis of pigmented skin lesions for formally trained dermatologists,” *Arch. Dermatol.*, vol. 131, no. 3, pp. 286–291, 1995.
- [14] J. Maeda, A. Kawano, S. Saga, and Y. Suzuki, “Number-driven perceptual segmentation of natural color images for easy decision of optimal result,” in *Proc. Int. Conf. Image Processing, 2007*, vol. 2, pp. 265–268.
- [15] J. Maeda, A. Kawano, S. Saga, and Y. Suzuki, “Unsupervised perceptual segmentation of natural color images using fuzzy-based hierarchical algorithm,” in *Proc. SCIA. New York: Springer, 2007*, vol. 4522, *Lecture Notes in Computer Science*, pp. 462–471.
- [16] G. McLachlan and T. Krishnan, *The EM Algorithm and Extensions*. New York: Wiley, 1997. [17] T. Mendonca, A. Marcal, A. Vieira, J. Nascimento, M. Silveira, J. Marques, and J. Rozeira, “Comparison of segmentation methods for automatic diagnosis of dermoscopy images,” in *Proc. IEEE Int. Conf. Engineering in Medicine and Biology Society, 2007*, pp. 6572–6575
- [17] Karray and de Silva “Soft Computing and Intelligent Systems Design” .Addison Wesley September 27, 2004.